

## Impurity states in grain boundaries and adjacent crystalline regions. II. Dynamic, electronic, and magnetic properties of crystalline regions adjacent to grain boundaries in metals

V. N. Kaigorodov, S. M. Klotsman, and S. N. Shlyapnikov

*Diffusion Phenomena Department, Institute of Metal Physics, Urals Division of the Russian Academy of Sciences, 620219 Ekaterinburg, Russia*

(Received 11 February 1992; revised manuscript received 29 April 1993)

Using a nuclear  $\gamma$ -resonance spectroscopy method we have investigated dynamic, electronic, and magnetic properties of one of the states localized in crystallites near the grain boundary. It has been shown that at high temperatures, at which the "intrinsic" properties of these states are conserved, isomeric shifts and dynamic properties of these states are identical to the corresponding values for the lattice sites of corresponding metals. At low temperatures, where "extrinsic" effects can manifest themselves, the properties of these states in gold do not change. But in other metals, in which rather high concentrations of interstitial impurities are possible, there is segregation of these impurities in the localization region of corresponding states, and, accordingly, there is a change of physical properties of these states. There are magnetic phase transitions in two-dimensional localization regions.

### I. INTRODUCTION

In Ref. 1, called I for short, we described the principles of a method for the investigation of the structure and properties of semimicroscopic one- and two-dimensional defects, such as dislocations and grain boundaries (GB's). In I, we presented emission nuclear  $\gamma$ -resonance spectra (NGRS), obtained after the introduction of atomic probes (AP's) by diffusion into polycrystalline metals. The phenomenological description of the AP relative state population  $\sigma$  in the GB diffusion (GBD) zone makes it possible to describe the temperature dependencies  $\sigma(\xi)$ , which define the "intensities"  $A_i$  of the NGR spectra components [ $\xi = (RT_{\text{diff}})^{-1}$ , where  $R$  is the gas constant and  $T_{\text{diff}}$  is the absolute temperature of diffusion introduction of AP's into the polycrystal]. The analysis of the temperature dependence  $\sigma(\xi)$  enabled us to establish microscopic mechanisms, defining the breaks in the GBD Arrhenius dependencies.

The dislocation pumping mechanism<sup>2</sup> arises and becomes predominant at low temperatures in pure matrices, when the productivity of AP pumping from the GB to the adjacent regions by means of volume diffusion becomes low, and if there are no segregation layers near the GB, containing strongly bonded vacancy-impurity complexes (VIC's). The next possible low-temperature pumping mechanism included in the phenomenological description of dependencies  $\sigma(\xi)$  (see I) is atomic-probe pumping from the GB to adjacent regions caused by vacancies, which enter into vacancy-interstitial-impurity complexes. The VIC concentration near the GB may be caused by residual interstitial impurities which diffuse from the bulk crystal to the vacancy sources, dislocations, and GB's. VIC's are formed, characterized by high bond energy. Their concentration is defined only by the interstitial-impurity concentration and VIC bond energy. In such a segregation layer, the pumping activation enthalpy of substitutional AP's is equal to the activation

enthalpy of vacancy migration, just as in the impurity region of self-diffusion in ionic crystals with polyvalent impurities.<sup>3,4</sup>

In this paper, on the basis of the classification of components of NGR spectra described in I, we present results of the investigation of dynamic, electronic, and magnetic properties of AP states, localized in the lattice sites adjacent to the GB.

### II. PROPERTIES OF THE AP STATES IN THE HIGH-TEMPERATURE RANGE

In Figs. 1–3 there are given as examples the typical NGR spectra of polycrystalline Pd, Pt, and Au, measured after different diffusion temperatures  $T_{\text{diff}}$ , which have been investigated in the most detail. At high  $T_{\text{diff}}$  (low values of  $\xi$ ) for AP diffusion introduction or AP redistribution between the states in the GBD zone there is only one line in NGR spectra, called line 1 for short. With increasing  $\xi$ , the area of this line 1 decreases in accordance with the phenomenological description of the temperature dependence of the state population  $\sigma(\xi)$  in the GBD zone, given in I.

In Table I we present some of the characteristic features of the  $\ln\sigma(\xi)$  dependence: the high- $\xi$  boundary of the intrinsic range of type-1 properties  $\xi_{\text{max}}^{\text{intr}}$ , the appearance temperature (AT) of line 2,  $\xi_{\text{AT}}$ , the intersection point (IP) of dependencies  $\sigma_1(\xi)$  and  $\sigma_2(\xi)$ ,  $\xi_{\text{IP}}$ . There we also present estimations of the pumping enthalpies  $Q_{\text{pump}}$ , defined at the appearance temperatures of NGRS component 2.

As can be seen, these characteristic features of Pd and Pt are situated at significantly higher values of  $\xi$  than  $\xi_{\text{max}}^{\text{intr}}$ . At the same time, for gold, the value of  $\xi_{\text{max}}^{\text{intr}}$  appears to be higher than magnitudes  $\xi_{\text{AT}}$  and  $\xi_{\text{IP}}$ . This shows the absence in Au of the interstitial-impurity segregation layer in lattice regions adjacent to the GB. This conclusion appears to be perfectly reasonable, if one

takes into account the small solubility of such impurities in gold. As was shown in I, according to the phenomenological description of dependencies  $\sigma(\xi)$ , the part of curve  $\sigma_2(\xi)$  for  $\xi < \xi_{IP}$  for gold can be described in the intrinsic approximation. Thus we will name this region of  $\xi$  values the high-temperature (high- $T_{diff}$ ) range, and the region of values  $\xi > \xi_{IP}$  the low-temperature (low- $T_{diff}$ ) region. According to this definition we will construct our further account.

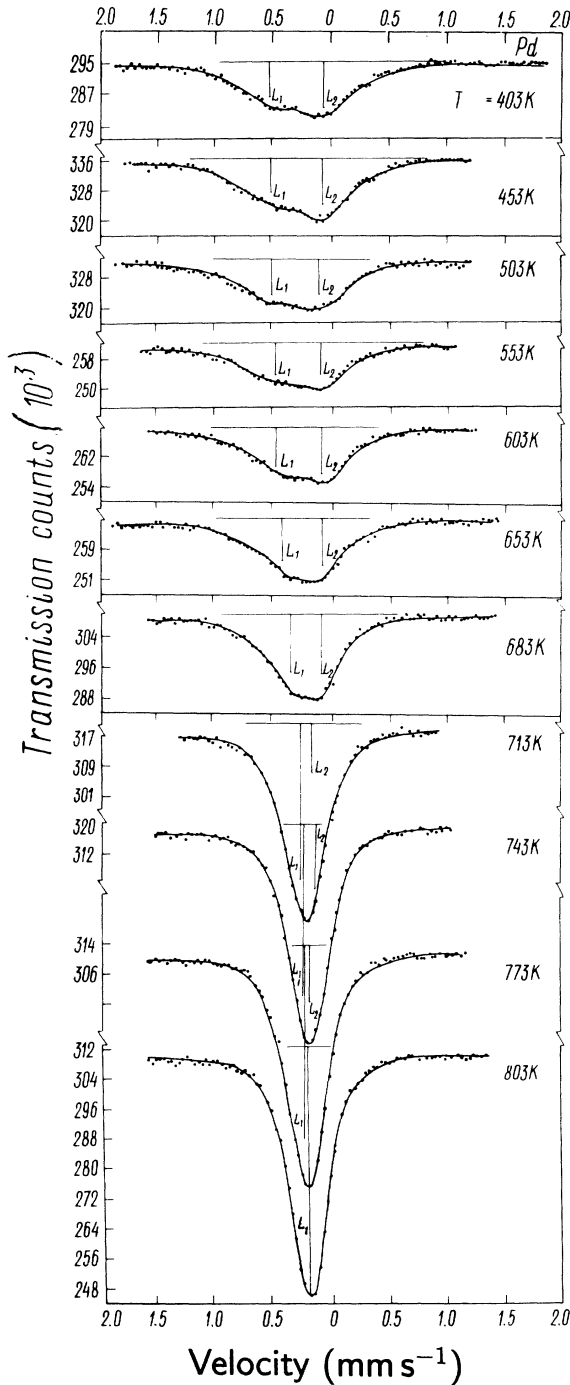


FIG. 1. Emission NGRS for polycrystalline Pd after annealing at different  $T_{diff}$ .

#### A. Type-1 properties in the high-temperature region

One of the most important characteristics of the components of the NGR spectra is the isomer shift (IS)  $\delta$ . As is known, the sign and the absolute value of  $\delta$  are determined by the difference between the  $s$ -electron density in the source (the investigated sample) and in the absorber of the NGR radiation. In our experiments we used the emission variant of NGRS with  $^{57}\text{Co}$  as the atomic probe. For our conditions a positive IS ( $0 < \delta$ ) means an increase of  $s$ -electron density at the AP nucleus in comparison with the  $s$ -electron density at the AP nucleus in iron.

Table II represents IS  $\delta_1^{HT}$  values, obtained from poly-

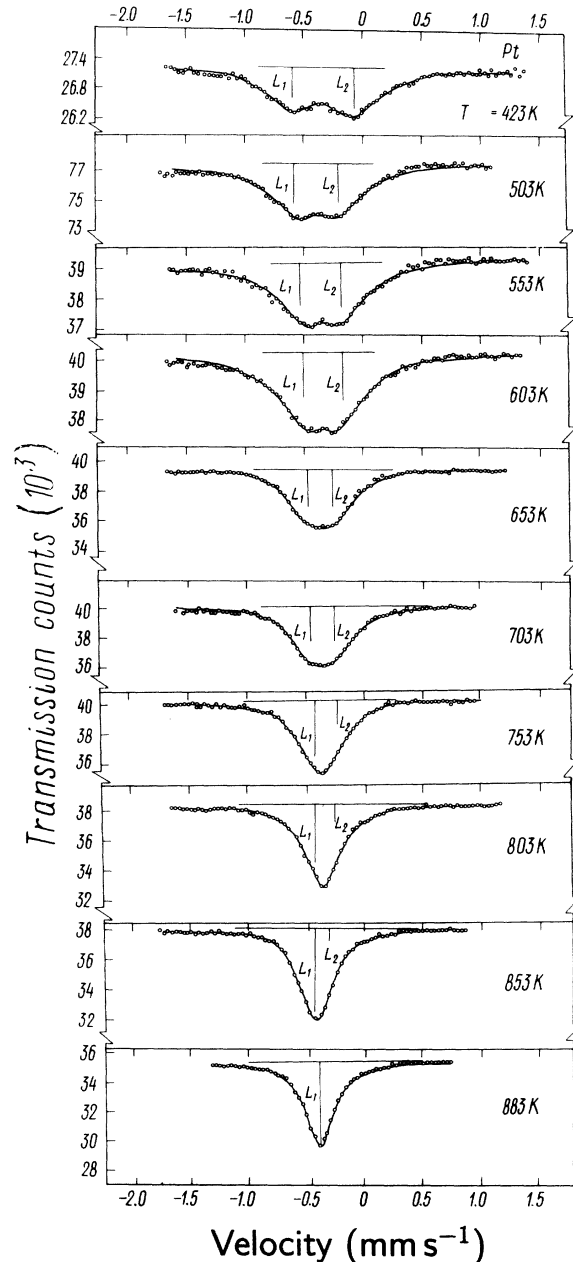


FIG. 2. Emission NGRS for polycrystalline Pt after annealing at different  $T_{diff}$ .

TABLE I. Theoretical estimations and experimental parameters of  $\sigma(\xi)$  dependencies for some fcc metals.

Parameters	Au	Pt	Pd
$Q(\text{Co})$ (kcal/mol) <sup>a</sup>	44.24	74.22	Fe:62.10
$D_0(\text{Co})$ (cm <sup>2</sup> /s) <sup>a</sup>	0.25	19.6	Fe:0.18
$10^4 \xi_{\text{max}}^{\text{intr}}$ [(kcal/mol) <sup>-1</sup> ]	8.7	5.8	6.0
$10^4 \xi_{\text{AT}}(\sigma_2)$ [(kcal/mol) <sup>-1</sup> ]	6.0	6.1	6.5
$10^4 \xi_{\text{IP}}$ [(kcal/mol) <sup>-1</sup> ]	6.3	7.3	7.5
$Q(\sigma_2)$ (kcal/mol) <sup>b</sup>	19.7	20.4	18.0
$Q_{\text{pump}}(\text{Co})$ (kcal/mol)	43.8	44.2	40.0

<sup>a</sup>Diffusion in Solid Metals and Alloys, edited by H. Mehrer, Landolt-Bornstein, Group 3, Vol. 26 (Springer-Verlag, Berlin, 1990).

<sup>b</sup>Determined from graphical slopes drawn by eye, so the errors of these values are unknown.

crystalline metals after high- $T_{\text{diff}}$  annealing. For comparison we present values of the IS  $\delta_{\text{refer}}$  from the literature. They were obtained either by measurements on single crystals or after high- $T_{\text{diff}}$  volume diffusion of AP's in polycrystals. Therefore, these data are the representative

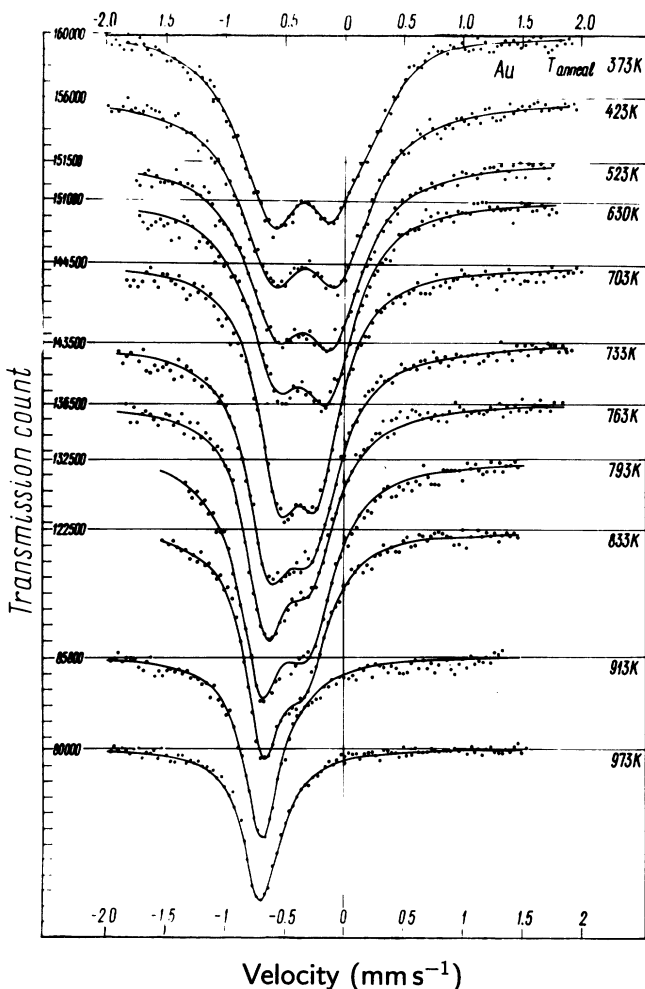


FIG. 3. Emission NGRS for polycrystalline Au after annealing at different  $T_{\text{diff}}$ .

TABLE II. Type-1 isomer shifts  $\delta_1^{\text{HT}}$  after high- $T_{\text{diff}}$  annealing and reference isomer-shift values  $\delta_{\text{refer}}$  for some fcc and bcc metals.

Matrix	$T_{\text{diff}}/T_{\text{melt}}$	$\delta_1^{\text{HT}}$ (mm/s)	$\delta_{\text{refer}}^a$ (mm/s)
V	0.44	+(0.07±0.02)	+(0.07±0.01)
Cr	0.41–0.51	+(0.12±0.01)	+(0.12±0.01)
Ni	0.42	–(0.07±0.02)	–(0.06±0.01)
Nb	0.39–0.53	–(0.03±0.01)	–(0.02±0.02)
Mo	0.49–0.54	–(0.09±0.01)	–(0.10±0.02)
Rh	0.38	–(0.24±0.03)	–(0.17±0.02)
Pd	0.40	–(0.22±0.02)	–(0.22±0.02)
Ta	0.45	–(0.07±0.01)	–(0.07±0.02)
W	0.27–0.40	–(0.18±0.01)	–(0.20±0.02)
Ir	0.35–0.39	–(0.31±0.03)	–(0.30±0.02)
Pt	0.40–0.47	–(0.40±0.03)	–(0.40±0.02)
Au	0.57–0.73	–(0.69±0.03)	–(0.67±0.02)

<sup>a</sup>T. A. Kitchens, W. A. Steyert, and R. D. Taylor, Phys. Rev. **138**, 467 (1968).

IS values for AP substitutional states in the regular lattice sites. The coincidence of measured values  $\delta_1^{\text{HT}}$  with values of  $\delta_{\text{refer}}$  enables us to infer that states of type 1 are the typical AP states in the regular lattice sites of those crystalline regions adjacent to the GB which are the AP pumping zone. (See Paper I for a definition of type-1 and type-2 states.)

Another important characteristic of the AP states is the Debye temperature  $\Theta$ . It is obtained from the dependence of the NGR probability (proportional to the absolute area value  $A_1$  of the NGRS component) on measuring temperature ( $T_{\text{meas}}$ ) of the NGR spectra. Figures 4–6 display as examples these dependences, measured on polycrystals of Pd, Pt, and Au. First of all, we notice the following qualitative result: at low  $T_{\text{meas}}$ ,  $A_1$  values deviate down from the dependencies  $\ln A_1(T_{\text{meas}})$  obtained at higher  $T_{\text{meas}}$ . This appears to contradict the theory of NGRS. To elucidate the reasons for such an anomaly, we carried out NGRS measurements in the compressed scale of the absorber velocities. In Figs. 7 and 8 we present NGR spectra measured at different  $T_{\text{meas}}$  in the compressed velocity scale. It is seen that at 5.5 K a

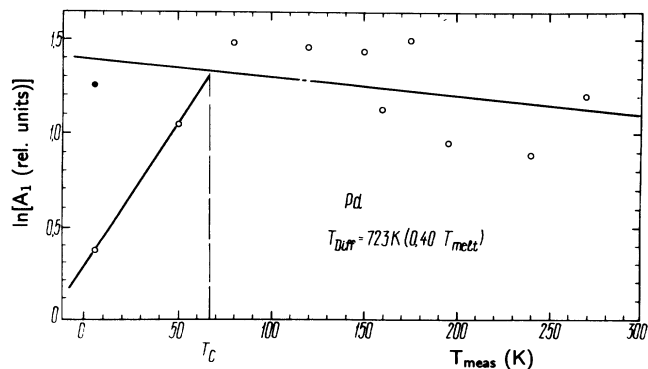


FIG. 4.  $\ln A_1(T_{\text{meas}})$  dependence for Pd annealed at high  $T_{\text{diff}}$ .

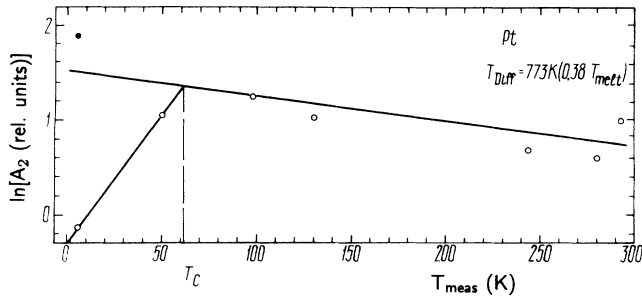


FIG. 5.  $\ln A_1(T_{\text{meas}})$  dependence for Pt annealed at high  $T_{\text{diff}}$ .

characteristic line sextet appears in polycrystals of Pd and Pt. This means that at low  $T_{\text{meas}}$  in the type-1 state localization region, magnetic ordering arises. The area of the whole sextet coincides with the area obtained by extrapolation of the high- $T_{\text{meas}}$  part of the dependence  $\ln A_1(T_{\text{meas}})$ . In Figs. 7 and 8 these values are marked by the filled symbols. We will discuss later the origin of the magnetic ordering in these matrices.

The Debye temperature values of the type-1 states,  $\Theta_1$ , were calculated by means of the expression

$$\Theta = 11.6 |\partial \ln A / \partial T_{\text{meas}}|^{-0.5}, \quad (1)$$

from the high-temperature parts of the curves  $\ln A_1(T_{\text{meas}})$ , because expression (1) is valid for  $T_{\text{meas}} > \Theta/2$ .

Table III represents the measured values  $\Theta_1^{\text{HT}}$  and values  $\Theta_{\text{refer}}$  obtained from the literature. It is obvious that agreement with previous data is satisfactory. This confirms once again the conclusion that the states of type 1 populated at high  $T_{\text{diff}}$  are the AP substitutional states in the lattice sites of the corresponding pure metals.

Let us turn now to the characteristics of magnetic ordering in type-1 state localization regions. As has been shown above, in Pd and Pt the magnetic field at the AP nucleus at low  $T_{\text{meas}}$  becomes so high that the single paramagnetic line is split into the characteristic sextet. In Au, Rh, and Ir the magnitude of the effective field at the AP nucleus is significantly lower, and we observed in these metals only a broadening of the single paramagnetic line at low  $T_{\text{meas}}$ .

Let us consider the results obtained on Pd and Pt in more detail. As is known,<sup>5</sup> in Pd and Pt magnetic order-

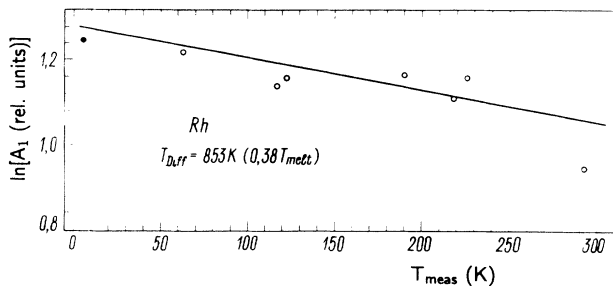


FIG. 6.  $\ln A_1(T_{\text{meas}})$  dependence for Rh annealed at high  $T_{\text{diff}}$ .

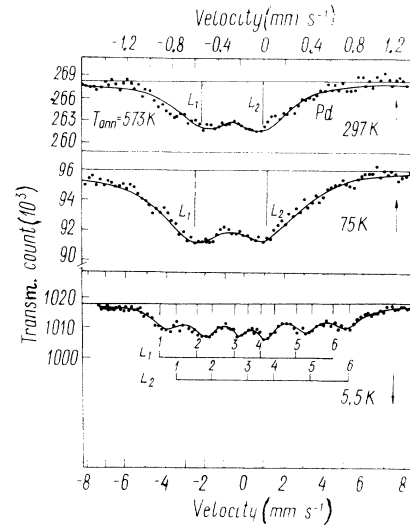


FIG. 7. NGR spectra for Pd measured at different  $T_{\text{meas}}$ .

ing occurs even in strongly diluted solid solutions of magnetically active impurities (MAI). The magnetic ordering in these dilute solutions is caused by an indirect-exchange mechanism, in which the conduction electrons of the matrix take an active part. The Curie temperature  $T_C$  in such strongly diluted solid solutions is defined by the expression<sup>5</sup>

$$T_C \propto C_{\text{MAI}} \chi_0 \propto C_{\text{MAI}} n^{1/3}. \quad (2)$$

Here  $C_{\text{MAI}}$  is the MAI concentration in the solid solution,  $\chi_0$  is the paramagnetic susceptibility, and  $n$  is the density of conduction electrons. Respectively, Table IV gives the values of Curie temperatures for type-1 states  $T_1^{\text{HT}}$ , the magnitudes of the effective magnetic fields at the AP nucleus  $H_1^{\text{HT}}$  and an estimation of the MAI concentration  $C_{\text{MAI}}$ . The last have been obtained by means of the well-known dependence  $T_C(C_{\text{MAI}})$ , measured by NGRS.<sup>6,7</sup>

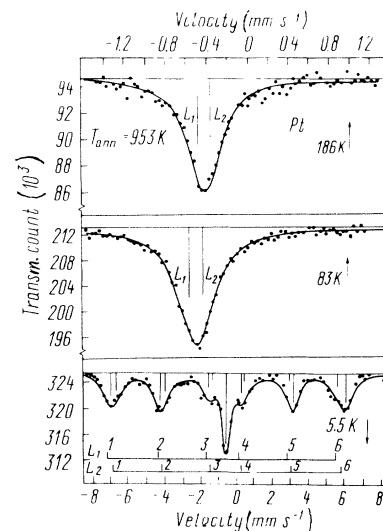


FIG. 8. NGR spectra for Pt measured at different  $T_{\text{meas}}$ .

TABLE III. Type-1 Debye temperatures  $\Theta_1^{\text{HT}}$  after high- $T_{\text{diff}}$  annealing for some fcc metals.

	Rh	Matrix Pd	Pt
$T_{\text{diff}}/T_{\text{melt}}$	0.38	0.37–0.40	0.38–0.47
$\Theta_1^{\text{HT}}$ (K)	(390±70)	(330±40)	(430±80)
$\Theta_{\text{refer}}$ (K) <sup>a</sup>	430	370	360

<sup>a</sup>W. A. Steyert and R. D. Taylor, Phys. Rev. **134**, 716 (1964). No errors are given, but typical errors in Debye-temperature determination by NGRS are  $\pm(20-50)$  K.

We wish to emphasize that  $3d$  impurities have a very high solubility in Pd and Pt. In addition, as has been shown theoretically and experimentally,<sup>8</sup>  $3d$  impurities in these metals do not segregate at the GB. Hence, there is no need to take into account the possibility of grouping of the MAI and AP. One can assume that MAI's were delivered to the pumping zone (region of type-1 state localization) during the introduction of AP by diffusion. However, the evident dependence of the magnitude  $T_1$  on metal purity (see Table IV) makes this assumption improbable.

Perhaps the reason for the residual MAI segregation is intrinsic oxidation.<sup>9</sup> But this hypothesis appears weak too. It would be necessary to segregate the residual MAI's from the whole crystalline volume at the GB, with MAI concentrations at the level of 1 at. % in a polycrystal with grain size of order  $10^{-2}$  cm and average concentration of substitutional impurities about 100 ppm. (Concentration of all the substitutional impurities in our samples was determined by secondary-ion mass spectrometry on ion microanalyzer IMS-3f, CAMECA, France and does not exceed 100 ppm in Pt and Pd.) But this is impossible. At  $T_{\text{diff}}$  on the lower boundary of the intrinsic region [for Pd and Pt  $\xi_{\text{max}}^{\text{intr}} \cong 6 \times 10^{-4}$  (kcal/mol)<sup>-1</sup>] the volume-diffusion coefficients are of the order of  $10^{-12}$  cm<sup>2</sup>/s. Within the time of AP diffusion introduction,  $t \cong 10^4$  s, they provide an effective diffusion depth for substitutional MAI's about  $X_D = (D_{\text{vol}} t)^{0.5} \cong 10^{-4}$  cm, which is two orders of magnitude smaller than the grain size in the polycrystals used.

Let us summarize the main result of this section. In all metals investigated by us, the NGRS parameters IS and Debye temperature, measured after annealing at  $\xi < \xi_{\text{IP}}$ , coincide exactly with the reference values. But it was established in I that for Pd and Pt the pumping characteris-

TABLE IV. Curie temperatures  $T_1^{\text{HT}}$  and effective magnetic fields  $H_1^{\text{HT}}$  of type-1 states after high- $T_{\text{diff}}$  annealing for Pd and Pt of different purities. HP indicates a high-purity sample, LP a low-purity sample.

Matrix	$T_{\text{diff}}/T_{\text{melt}}$	$T_1^{\text{HT}}$ (K)	$H_1^{\text{HT}}$ (kOe)	$C_{\text{MAI}}$ (at. %)
Pd HP	0.40	70±10	293±2	2
Pd LP	0.42	270±20	290±3	> 10
Pt HP	0.38	110±10	316±2	5
Pt LP	0.42	200±20	315±3	> 20

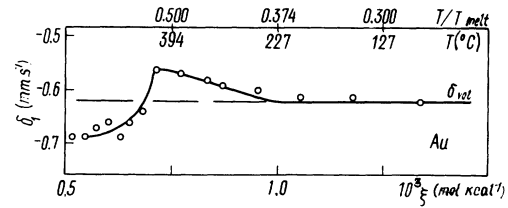


FIG. 9. Dependence of IS,  $\delta_1(\xi)$ , for polycrystalline Au.

tics do not coincide with the volume-diffusion parameters. Apparently, concentration of the interstitial impurities and VIP's in the pumping zone is low till  $\xi_{\text{IP}}$ . One may think that as the AP introduction temperature  $T_{\text{diff}}$  decreases, the concentration of interstitial impurities in the pumping zone will increase. This will lead to the changes of NGRS parameters already observed. The magnetic phase transition which was discovered in the localization zone of AP type-1 states presents an additional tool for investigation of the properties of these regions.

### B. Type-1 properties at low temperatures

In the previous section we discussed the nature and properties of states of type 1, which the AP's occupy during high- $T_{\text{diff}}$  annealing, at  $\xi < \xi_{\text{IP}}$ . In these conditions, the relative type-1 state population  $\sigma_1$  changed rapidly with a change of  $T_{\text{diff}}$ . However, these changes no longer occur at low  $T_{\text{diff}}$ , at  $\xi_{\text{IP}} < \xi$ . The independence of the NGRS components on  $T_{\text{diff}}$  means that, in the corresponding temperature range  $\xi_{\text{IP}} < \xi$ ,

$$Q_{\text{pump}}^{\text{LT}} \cong Q_{\text{GB}}. \quad (3)$$

This expression has been already introduced in I in the discussion of the macroscopic GBD properties, in connection with the introduction of a new pumping mechanism to explain the break in the Arrhenius dependence of the GBD parameter  $W(\xi)$  or  $\mathcal{E} = \alpha^{5/3} t^{0.5}$  (see I).

As has been shown in I, the character of the  $\sigma(\xi)$  dependence can be described if one uses the natural notion that at rather low  $T_{\text{diff}}$  there appears a segregation layer of interstitial impurities near the GB. It is natural

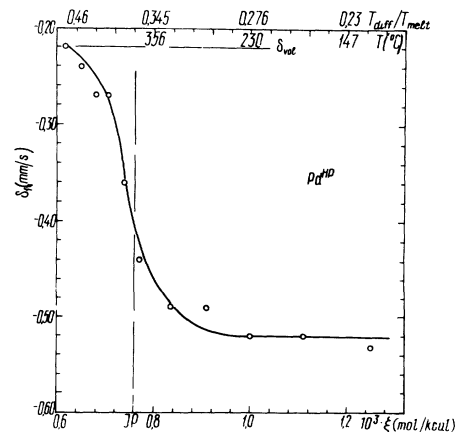
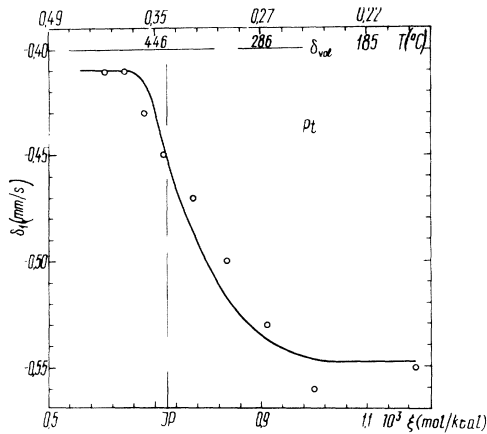


FIG. 10. Dependence of IS,  $\delta_1(\xi)$ , for polycrystalline Pd.

FIG. 11. Dependence of IS,  $\delta_1(\xi)$ , for polycrystalline Pt.

that rather strong doping by segregated impurities of the pumping zone must change the NGRS parameters of the AP's which occupy this zone.

Let us consider the IS magnitudes  $\delta_1$  measured after low- $T_{\text{diff}}$  annealings. In Fig. 9 is shown the  $\delta_1(\xi)$  dependence for Au. As is seen, the IS for type-1 states,  $\delta_1$ , practically does not change and at lowest  $T_{\text{diff}}$  is fulfilled by  $\delta_1 = \delta_{\text{vol}}$ . This result is an excellent confirmation of the conclusion, made in Paper I and in the Introduction of this paper, that in Au, owing to the negligibly small volume solubility of the interstitial impurities, segregation of these interstitial impurities near the GB does not occur. There is also one more important point to be made: at the lowest- $T_{\text{diff}}$  annealing for AP introduction, there appear no new AP states different from those which were identified after high- $T_{\text{diff}}$  annealing. This conclusion will help in the analysis of the dependencies  $\delta_1(\xi)$  of the other polycrystalline metals.

In Figs. 10 and 11 the dependencies  $\delta_1(\xi)$  for Pt and Pd are presented. The dashed lines mark the position of  $\xi_{\text{IP}}$ . As is seen here, unlike the case of Au, a fast decrease of the IS takes place after  $\xi_{\text{IP}}$ . This confirms to a certain degree the introduction of the  $\xi_{\text{IP}}$  value as a boundary for the region of intrinsic properties of type 1. To explain the results represented in Figs. 10 and 11, let us use the consequences of our hypothesis on the doping of the type-1 localization region at low  $T_{\text{diff}}$  by the interstitial impurities and their VIC's.

It is known that doping of the metal volume by substitutional impurities changes the NGRS parameters only slightly.<sup>10</sup> Thus, doping Pt with 20 at. % of Fe induces no changes of the IS of the  $^{57}\text{Co}$  paramagnetic line. This means that neither the occurrence of the majority of the

TABLE V. IS changes after different diffusion annealings, IS barometric coefficients for Pd and Pt, and estimated interstitial-impurity concentrations  $C_{\text{diff}}^{\text{II}}$ .  $\delta_1(\text{LT,HT}) = \delta_1(\text{low } T_{\text{diff}}) - \delta_1(\text{high } T_{\text{diff}})$ .

	$\delta_1^{\text{LT}}$	$\delta_1^{\text{HT}}$	$\delta_1(\text{LT,HT})$	$V(\partial\delta/\partial V)$	$C_{\text{diff}}^{\text{II}}$
	$\pm 0.01$	$\pm 0.02$			$(\text{at. } \%)$
	(mm/s)	(mm/s)	(mm/s)	(mm/s)	
$T_{\text{diff}}/T_{\text{melt}}$	0.22	0.40			
Pd	-0.50	-0.22	-0.28	-0.60	0.5
Pt	-0.60	-0.42	-0.18	-0.40	0.3

substitutional impurity nor vacancy segregation in the pumping zone can lead to changes in the NGRS parameters. Thus, we can limit our consideration to the interstitial impurities only.

It is known that interstitial impurities increase the lattice parameters of metals. This means that the value of the atomic volume per lattice site increases in a solid solution with interstitial impurities. Therefore, AP's in type 1 after low- $T_{\text{diff}}$  annealing appear to occupy sites with effectively increased volumes. The IS change produced is opposite in sign to the IS changes which occur at the high pressure. In Table V we present the differences  $\delta_1^{\text{LT}} - \delta_1^{\text{HT}} = \delta_1(\text{LT,HT})$  and the IS barometric coefficients for Pd and Pt.<sup>11</sup> The negative sign of the derivative  $\partial\delta/\partial V$  means that the atomic-volume growth in Pd and Pt is accompanied by an IS decrease for  $^{57}\text{Fe}$ . The absolute value  $V(\partial\delta/\partial V)$  for Pd is 1.5 times greater than that for Pt, in accordance with the difference ratio  $\delta_1(\text{LT,HT})$  for these metals.

We will use the experimentally established isomer-shift dependence for  $^{181}\text{Ta}$  in Ta and  $^{57}\text{Fe}$  in Pd on the concentration of the classical interstitial impurity, hydrogen.<sup>12,13</sup> In agreement with the measured IS barometric coefficient in Ta,<sup>11</sup> the IS decreases linearly at the rate  $\partial\delta/\partial C(\text{H}) = -57 \text{ mm/s at. } \%$  H in the Ta(H) system.<sup>12</sup>

From data presented in Figs. 10 and 11, we can estimate the concentration of the interstitial impurities in the pumping zone. For this estimation we use the value of  $\partial\delta/\partial C(\text{H})$  measured in the Ta(H) alloy as a minimum value for the IS changes for the interstitial impurities in Pd and Pt. Table V presents the corresponding maximum estimations of interstitial-impurity concentrations. As can be seen in the pumping zone, the interstitial-impurity concentration does not exceed 0.5 at. %, which seems reasonable if one takes into account that the solubility of carbon in Ni and Pt, for example, reaches 2 at. %.<sup>14,15</sup>

In Figs. 12–14 we show the dependencies of the line-1

TABLE VI. Debye temperatures  $\Theta_1^{\text{LT}}$  of type-1 states after low- $T_{\text{diff}}$  annealing for some fcc metals.

	Metal				
	Rh	Pd	Ir	Pt	Au
$T_{\text{diff}}/T_{\text{melt}}$	0.30	0.24	0.25	0.21	0.32
$\Theta_1^{\text{LT}}$ (K)	(240±20)	(300±40)	(350±90)	(250±25)	(320±30)
$(\Theta_1^{\text{LT}} - \Theta_1^{\text{HT}})_1$ (K)	-(150±90)	-(0±80)		-(120±110)	
$\Theta_{\text{refer}}$ (K)	430	370	460	360	330

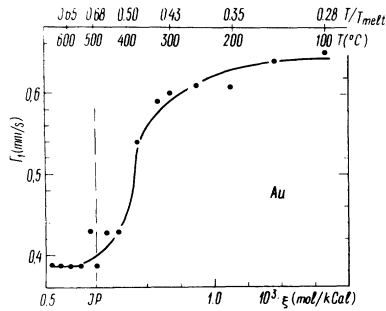


FIG. 12. Dependence of FWHM  $\Gamma_1(\xi)$ , for polycrystalline Au.

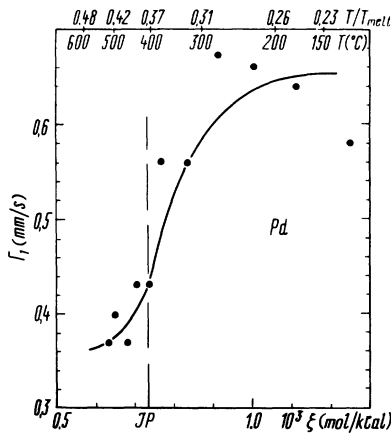


FIG. 13. Dependence of FWHM  $\Gamma_1(\xi)$ , for polycrystalline Pd.

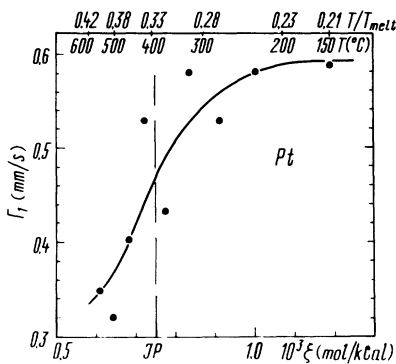


FIG. 14. Dependence of FWHM  $\Gamma_1(\xi)$ , for polycrystalline Pt.

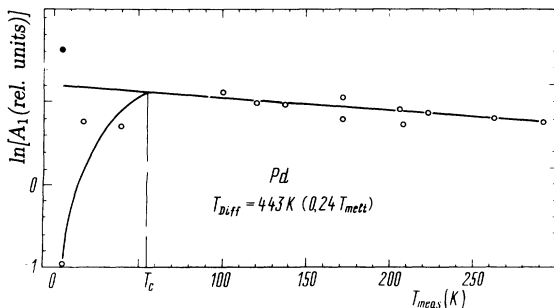


FIG. 15.  $\ln A_1(T_{\text{meas}})$  dependence for Pd annealed at low  $T_{\text{diff}}$ .

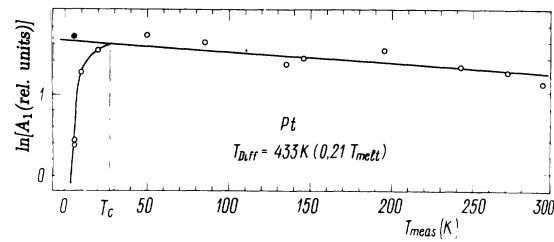


FIG. 16.  $\ln A_1(T_{\text{meas}})$  dependence for Pt annealed at low  $T_{\text{diff}}$ .

full width at half maximum (FWHM)  $\Gamma_1(\xi)$ . As is seen,  $\Gamma_1$  changes analogous to the IS change:  $\Gamma_1 = \Gamma_{\text{refer}}$  at high  $T_{\text{diff}}$ , and after  $\xi_{\text{IP}}$  the  $\Gamma_1$  value changes rapidly, appearing to become saturated in the low- $T_{\text{diff}}$  range. Just the same dependence of  $\Gamma$  on hydrogen concentration  $C(\text{H})$  was observed in solid solutions Ta(H) in Ref. 12. Such a dependence is explained by the existence of interstitial impurities (in our case VIC's) around the AP, which leads to a set of AP states, with similar properties. In Au the increase of  $\Gamma_1$  with  $\xi$  is also observed, although  $\delta_1(\text{LT})$  in Au is nearly constant and equal to  $\delta_{\text{refer}}$ .

Let us turn now to the consideration of dynamic properties of states of type 1 at low  $T_{\text{diff}}$ . Figures 15–17 display a  $\ln A_1(T_{\text{meas}})$  dependence in which the magnetic anomaly is shown clearly. The normal value of  $A_1$  (5.5 K) is restored after taking into account the areas of all sextet lines. The dynamic parameters calculated from Eq. (1) are given in Table VI. As can be seen, only for Rh and Pt does it appear that  $\Theta_1^{\text{LT}} < \Theta_1^{\text{HT}}$ ; in Pd  $\Theta_1^{\text{LT}} \cong \Theta_1^{\text{HT}}$ . For an explanation of such behavior it is necessary to identify the interstitial impurity in each metal.

The parameters of the magnetic transformation after low- $T_{\text{diff}}$  annealing are given in Table VII. They cannot be compared with corresponding values measured after high- $T_{\text{diff}}$  annealing. As we pointed out, the source of interstitial impurities entering the sample is not established, and this prevents comparison in detail of the magnetic characteristics of AP type 1 after different annealings.

However, the halving of  $T_1^{\text{LT}}$  after low- $T_{\text{diff}}$  annealing is a reliable result. As is known,<sup>16</sup> doping by interstitial impurities (like O and B) of bulk Pd, and very likely Pt, leads to a decrease of the density of states at the Fermi surface and to a  $T_C$  decrease. One may think that it is

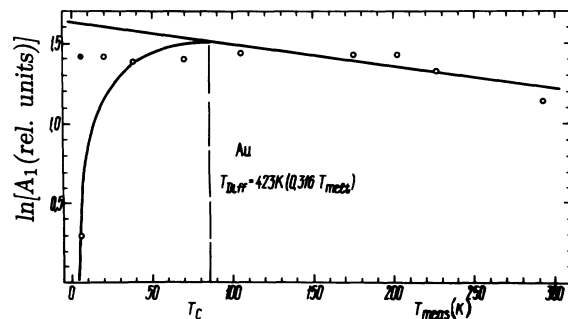


FIG. 17.  $\ln A_1(T_{\text{meas}})$  dependence for Au annealed at low  $T_{\text{diff}}$ .

TABLE VII. Curie temperature  $T_1^{LT}$  and effective magnetic fields  $H_1^{LT}$  for type-1 states after low- $T_{diff}$  annealing for some fcc metals.

Matrix	$T_{diff}/T_{melt}$	$T_1^{LT}$ (K)	$H_1^{LT}$ (kOe)
Pd	0.24	47±5	270±4
Pt	0.21	30±3	262±2
Rh	0.30	100±20	190±2
Ir	0.25	100±30	60±3
Au	0.32	20±5	270±2

the same effect which is observed in the type-1 localization zone in interstitial-impurity segregation at low  $T_{diff}$ .

### III. CONCLUSION

The method created in I was used to measure the properties of states of type 1, localized in the pumping zone near the GB. In Au, in which the bulk interstitial-impurity solubility is low, a high-purity matrix is created. In this condition, type-1 properties even after the lowest

$T_{diff}$  annealings coincide with lattice-site properties.

In Pd and Pt the properties of type-1 states coincide only in the high- $T_{diff}$  range with the properties of lattice sites. With decrease of  $T_{diff}$  the IS in Pd and Pt decreases, which shows the decrease of  $s$ -electron density at the AP nucleus. These IS changes are caused by the segregation of interstitial impurities, which causes an increase in the lattice parameter, and leads to the decrease of the concentration of self- $s$ -electrons and conduction  $s$ -electrons in the region of AP localization.

NGRS parameters of type-1 states in fcc metals completely confirm the classification of NGRS components described in I on the basis of  $\sigma(\xi)$  dependence, and create a base for analysis of physical properties of new AP states, localized in the GB core. The following paper<sup>17</sup> will be devoted to an account of these results.

### ACKNOWLEDGMENTS

The authors thank Professor S. V. Vonsovskii for support and useful discussions.

<sup>1</sup>V. N. Kaigorodov and S. M. Klotsman, preceding paper, Phys. Rev. B **49**, 9376 (1994).

<sup>2</sup>V. N. Kaigorodov *et al.*, Fiz. Met. Metaloved. **27**, 627 (1969).

<sup>3</sup>A. Lidiard, in *Ionic Conductivity*, edited by S. Flugge (Springer-Verlag, Berlin, 1957), p. 165.

<sup>4</sup>N. L. Peterson and S. J. Rothman, Phys. Rev. **177**, 1329 (1969).

<sup>5</sup>S. V. Vonsovskii, in *Magnetism*, edited by A. A. Gusev (Nauka, Moscow, 1971), p. 629.

<sup>6</sup>W. Trousdale and G. Longworth, J. Appl. Phys. **38**, 922 (1967).

<sup>7</sup>J. Crangle and W. R. Scott, J. Appl. Phys. **36**, 921 (1965).

<sup>8</sup>S. Mukherjee *et al.*, Surf. Sci. **188**, L742 (1987).

<sup>9</sup>*Oxydation des Metaux*, edited by J. Benard (Gauthier-Villars,

Paris, 1962).

<sup>10</sup>G. Bemski *et al.*, Phys. Lett. **18**, 213 (1965).

<sup>11</sup>R. Ingals *et al.*, Phys. Rev. **115**, 165 (1967).

<sup>12</sup>J. S. Carlow and R. E. Meads, J. Phys. F **2**, 982 (1972).

<sup>13</sup>A. Heidemann *et al.*, Phys. Rev. Lett. **36**, 213 (1976).

<sup>14</sup>C. Kostler, F. Faupel, and T. Hehencamp, Scr. Metall. **20**, 1755 (1986).

<sup>15</sup>U. Dahmen *et al.*, Metall. Trans. A **17**, 807 (1986).

<sup>16</sup>T. Auerswald *et al.*, Phys. Rev. B **43**, 14 232 (1991).

<sup>17</sup>V. N. Kaigorodov and S. M. Klotsman, following paper, Phys. Rev. B **49**, 9395 (1994).